2012 International Symposium on Computer, Consumer and Control

Adaptive Beam Steering Smart Antenna System for Ultra-High-Frequency Radio Frequency Identification Applications

Ting-Jui Huang and Pei-Hsuan Pan
Department of Communications Engineering
Yuan Ze University
ChungLi, Taiwan
s1008604@mail.yzu.edu.tw;
s1004828@mail.yzu.edu.tw

Heng-Tung Hsu
Department of Communications Engineering
Communication Research Center
Yuan Ze University
ChungLi, Taiwan
htbeckhsu@saturn.yzu.edu.tw

***Abstract*— Smart antenna technologies have been widely applied in many wireless communication systems due to performance enhancement in terms of data range, coverage and capacity. Up to now, not much effort was devoted for ultra high-frequency (UHF) radio frequency identification (RFID) applications mainly due to the relatively large size of the antenna element. In this paper, we present a compact-sized electrically steerable parasitic array radiator antenna (ESPAR) as the antenna element for UHF band. The proposed antenna featured 5.2 dBi peak gain with 100^o 3-dB beamwidth in broadside direction. Integrated with the control network composed of p-i-n diodes, the proposed smart antenna system is capable of providing complete coverage in the azimuthal direction.**

Keywords-smart antenna; ultra high-frequency; radio frequency identification; steerable; array.

I. INTRODUCTION

Radio frequency identification (RFID) is rapidly developing technology which is widely adopted for various data collection applications such as warehouse and retail item management [1,2]. Currently, several frequency bands have been assigned to RFID applications, such as 125 kHz, 13.56 MHz, 840~960 MHz, 2.45GHz, and 5.8 GHz. The Microwave RFID band 2.45 GHz is allocated around the frequency range from 2.4GHz to 2.4835 GHz. Compared to the UHF RFID systems around 900 MHz, the 2.45 GHz systems have the advantages of compactness, flexibility, and maneuverability for the item management applications.

Smart antenna technologies have been widely applied in a lot of communication systems. Such technologies basically consist of reconfigurable antennas, control networks to realize beam-forming functionality, and software for signal processing. Lots of successful implementations have proven the capability of smart antenna systems on performance enhancement in terms of coverage, range, data rate, capacity, and flexibility [3,4]. With the great success in the application of smart antennas for communication systems, not much of the work has been reported at UHF RFID frequencies. Yu [5] demonstrated an anti-collision algorithm based on smart antenna in RFID system and showed a 50 percent improvement in terms of the tag reading rates. Similar performance enhancement was also addressed in [6].

The antenna structures play a significant role in smart antenna systems. Generally speaking, antenna arrays with control networks are implemented to realize the beam steering feature. One of the major reasons in the lack of UHF RFID smart antenna is the fact that the wavelength at UHF frequency band is relatively long making the antenna arrays unrealistically bulky. In [6], the overall size of the antenna array was 3 cm × 50 cm × 50 cm with complicated beam forming network to realize both azimuth and elevation bean scanning. Apparently, size reduction and ease-of-implementation solutions are critical for large scale implementations.

The electronically steerable parasitic array radiator (ESPAR) antenna was widely applied in smart antenna systems due to its unique feature of being relatively easy to direct the radiation at intended recipients [7-9]. In general, the parasitic elements in the ESPAR can be terminated or loaded with various reactive loads to synthesize very complicated radiation patterns for complex system applications [10,11]. Compared to other adaptive beam forming antenna systems, such realization is believed to be simple and cost effective in terms of real implementations.

In this paper, we presented a compact-sized ESPAR structure as the antenna element for UHF RFID smart antenna system. The beam steering network was realized using p-i-n diodes and integrated with the radiating elements for cost-effective purpose. Through proper settings assigned by the microcontroller, the smart antenna system provided a complete coverage in the azimuthal direction in one of the operation modes.

II. SYSTEM ARCHITECTURE AND OPERATIONS

Fig. 1 shows the system architecture of the UHF RFID smart antenna system composing of a steerable antenna, beam steering network (BSN) with embedded microcontroller unit (MCU), RFID reader and personal computer with database. The steerable antenna structure is composed of a main radiator together with parasitic elements connected to ground plane through p-i-n diodes. The beam forming network is implemented using programmable microcontroller which sends the bias settings to switch the p-i-n diodes ON and OFF. Each combination of the bias setting corresponds to a “state” and the entire azimuth plane is divided into six states spatially. In other words, the

978-0-7695-4655-1/12 $26.00 © 2012 IEEE
DOI 10.1109/IS3C.2012.185

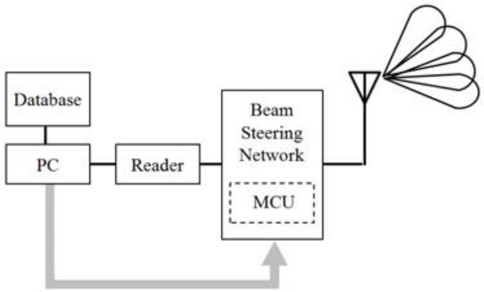

Figure 1. System architecture of the proposed smart antenna for UHF RFID applications

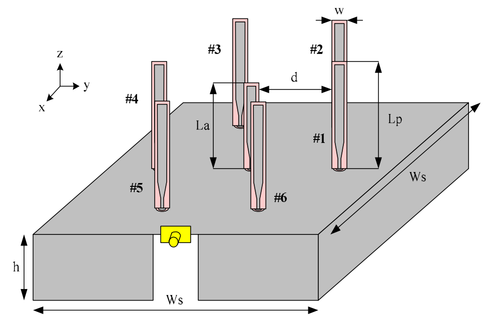

Figure 2. Geometry of the proposed antenna designed on 0.8mm FR4 substrate with ground skirt

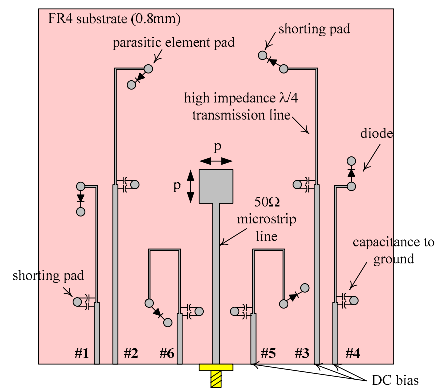

Figure 3. The details of BSN implemented on the backside of the ground plane including the high ipedance lines as RF chokes with bypass caps.

main lobe direction of each state is 60 degrees apart from each other. The operation of the system starts with the "pre-scan" mode in which the antenna beam is switched sequentially covering the entire azimuth plane. Information of all the detectable tags in the field will be stored in the database for further processing.

For "query" mode of operation, the BSN keeps sending sequential signal to steer the antenna beams from state to state, and the tags detected each cycle are pushed into the database for comparison with the data stored from last cycle. Notification of difference between consecutive cycles will be broadcasted to system users and the database always keeps the most updated tag list. For "tracking" mode of operation, list of the tags to be tracked will be preloaded into the database before pre-scan starts. Tag information collected at the pre-scan mode will be compared against the database and the corresponding state(s) that matches the preloaded tag list will be recorded. Then the PC sends commands to BSN and sets the antenna patterns in a sense to continuously track the desired tags. Combination of the operation modes certainly offers flexibility for practical application scenarios.

III. Implementation of Antenna and Beam Steering Networks (BSN)

Fig. 2 shows the detailed configuration of the proposed antenna to be implemented on an FR-4 substrate with a thickness of 0.8mm and dielectric constant of 4.2. As is shown in Fig. 2, the center element and the parasitic elements are designed to be monopole antennas sharing the common ground plane. To simplify the excitation configuration of the antenna, we adopted the microstripline on the backside of the ground plane as the feed to the center radiator. The BSN, shown in Fig. 3, composed of p-i-n diodes (part number SMS7621 from Skyworks, Inc.) was also implemented on the backside of the ground plane to make the overall antenna structure compact and cost-effective at the same time.

With the diodes connected between the ground plane and the parasitic elements, the parasitic elements are connected to either short-circuit (diodes ON) or open-circuit (diodes OFF) loads through the proper control of the individual bias voltages. High impedance quarter-wavelength transmission lines at the design frequency are included acting as RF chokes to suppress possible RF leakage to the DC bias which in turn will degrade the overall antenna performance. Table I summarizes the physical dimensions of the antenna designed at 915MHz.

The main principle of operation lies in the control of the loads connected to the parasitic elements. In general, when

TABLE I. Physical Dimensions of the Antenna Designed at 915MHz

La	Lp	Ws	w	d	h	p
77 mm	96 mm	150 mm	10 mm	60 mm	40 mm	10 mm

TABLE II. Bias Settings for the Six States of Steerable Antenna Structure

	#1	#2	#3	#4	#5	#6
State 1/0°	off	off	**on**	**on**	**on**	off
State 2/60°	off	**on**	**on**	**on**	off	off
State 3/120°	**on**	**on**	**on**	off	off	off
State 4/180°	**on**	**on**	off	off	off	**on**
State 5/240°	**on**	off	off	off	**on**	**on**
State 6/300°	off	off	off	**on**	**on**	**on**

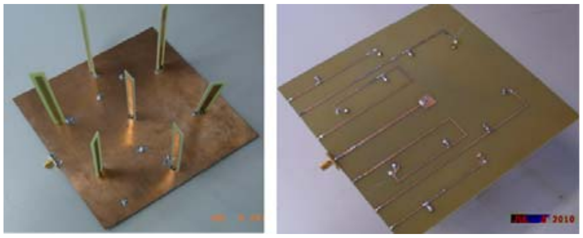

Figure 4. Fabricated prototype of the steerable antenna on FR4

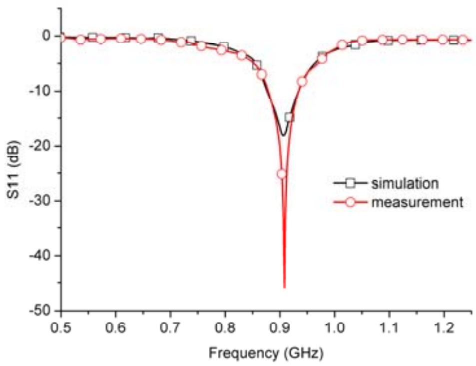

Figure 5. Simulated and measured S_{11} of the prototype set at "State 1"

the parasitic element is shorted to ground, it acts like a reflector. On the contrary, when the parasitic element is connected to open-circuit load, it acts like a director. Thus, the steering of the main beam can be achieved through the control of the ON/OFF behavior of the diodes connected to the parasitic elements. For our specific application scenario, the complete azimuth coverage of 360 degrees is divided into six sectors with a coverage of 60 degrees per sector. For convenience purpose, each sector is then referred to as a "state". The main beam can be directed into any one of the six states according to the settings of the bias voltages listed in Table II. The "on" state voltage for the diode is set at 1V.

IV. Results and Discussions

Fig.4 shows the picture of the fabricated prototype at 915 MHz. CST Studio Suite™ was used as the primary simulation tool. In order to evaluate the effect of p-i-n diodes precisely, the S-parameters of the diodes at ON and OFF states were measured first and integrated for complete system simulation. Fig.5 shows the simulated and measured S_{11} of the prototype set at "State 1". It is clear that the measurement agrees well with the simulation. We obtained similar results for all the other states. Fig.6(a) shows the simulated radiation pattern at 915 MHz on the x-y plane for the six states. It is observed that the main beam can be directed to the pre-defined azimuth position as desired. The simulated gain is around 5.5dB peaked at main beam direction. Fig. 6(b) shows the measured radiation patterns. As is observed in Fig. 6(b), the main beam tends to direct to

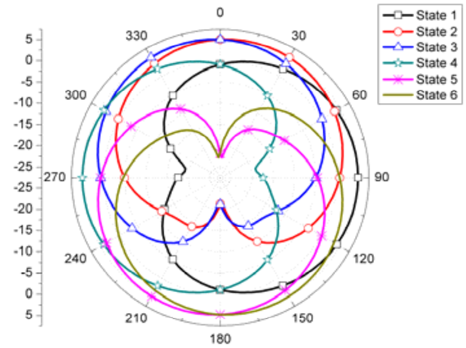

(a)

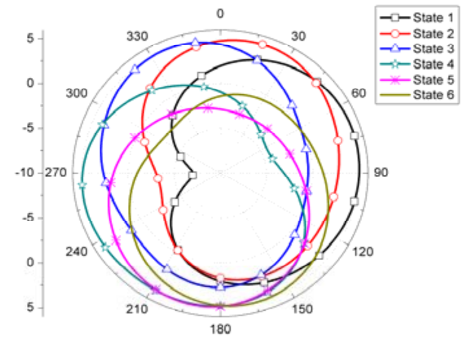

(b)

Figure 6. (a)Simulated and (b) measured farfield radiation patterns for the

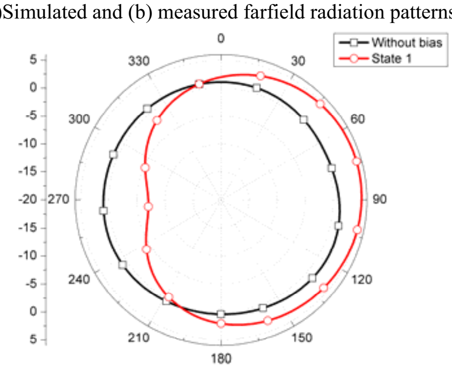

Figure 7. Comparison of the farfield radiation pattern between "State 1" and the case when all the diodes are off

a slight elevation angle of 30° which can be further suppressed by increasing the height of the ground skirt. The measured gain is 5.1dB with a 3dB beam width of 86 degrees. Despite the measurement exhibited a slightly wider beam width than the simulated one, the agreement between the simulation and measurement was quite well in general. The widening in beam width for the measurement was mainly due to the wires connecting the power supply to the antenna. Fig. 7 shows the comparison of the farfield radiation patterns between "State 1" and the case when all the diodes were biased at OFF state. The directive feature of

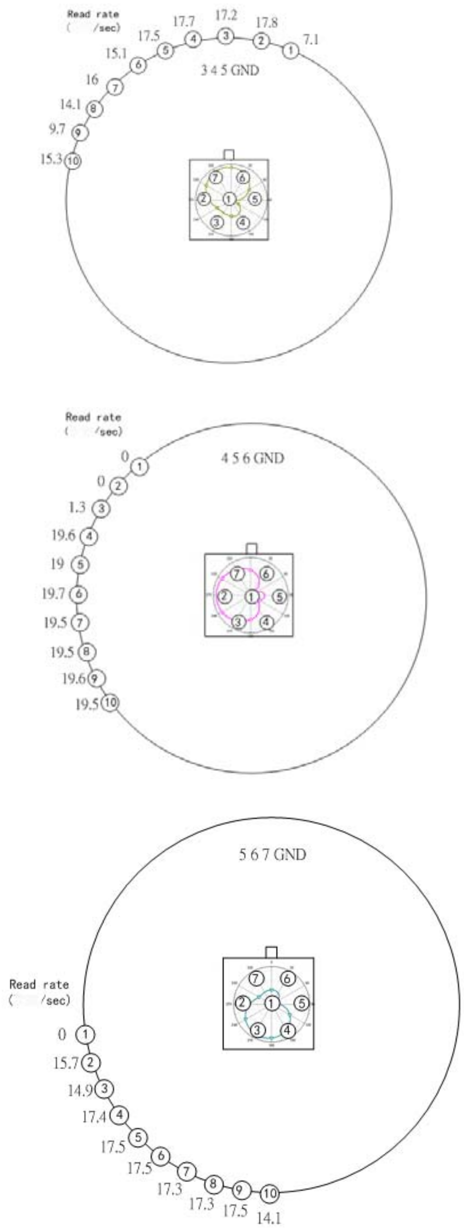

Figure 8. Capture of the readrates for state 1 (top), state 3 (middle) and state 4 (bottom) when the system is in query mode.

the antenna is again verified through the difference from the patterns.

The fabricated antenna element together with integrated BSN was then integrated into the complete system for complete performance test in anechoic chamber. The reader adopted was UHF Gen2 Speedway IPJ-R1000 Reader from Impinj^{TM}. With the reader output power set at 30dBm corresponding to 3.2Watt EIRP, the maximum read range of a single tag for the system was 4.2m. The system was then set to operate in the "query" mode where the antenna was kept steering from state to state. The time frame set for each state was 5 seconds. With the tags lined up along a circle of radius 1.5m and antenna at the center, Fig. 8 shows the captured read rate for state 1, state 3 and state 4, respectively. Clearly, the spatial distribution of the locations of readable tags agreed with the antenna pattern very well.

V. CONCLUSION

This paper presents a complete implementation of a smart antenna system for UHF RFID applications. The demonstrated prototype was fabricated on 0.8mm FR4 substrate and the beam steering network was integrated nicely with the antenna structure. The measurement results agreed well with simulation demonstrating complete functionality of the system. To the authors' best knowledge, this is one of the very few complete UHF RFID smart antenna system ever reported.

REFERENCES

[1] Daniel M. Dobkin, The RF in RFID, Newnes, 2007.

[2] Klaus Finkenzeller, RFID Handbook: Fundamentals and Applications in Contactless Smart Cards and Identification, 2nd ed., John Wiley & Sons Ltd, 2003.

[3] Lei Zan, Syed Ali Jafar, Combined Opportunistic Beamforming and Receive Antenna Selection. IEEE Comm Society, pp. 1007-1011, 2005.

[4] J. Butler and R. Lowe, "Beam-Forming Matrix Simplifies Design of Electronically Scanned Antennas," Electronic Design, pp. 170-173, April 12, 1961.

[5] J. Yu, K. H. Liu, X. Huang,and G. Yans, "An Anti-collision Algorithm Based on Smart Antenna in RFID Systems," Proceedings of the 2008 International Conference on Microwave and Millimeter Wave Technology, ICMMT 2008.

[6] N. C. Karmakar, S. M. Roy and M. S. Ikram, "Development of Smart Antenna for RFID Reader," 2008 IEEE International Conference on RFID, pp. 65-72.

[7] R.Schulb, J.Lu, and T. Ohira, "Seven-Element Ground Skirt Monopole ESPAR Antenna Design From a Genetic Algorithm and the Finite Element Method", IEEE Transactions on Antennas and Propagation, vol. 51, No. 11, pp. 3033-3039, Nov. 2003.

[8] J.Cheng,M.Hashiguchi, K.Ligusa, and T.Ohira,"Electronically steerable parasitic array radiator antenna for omni- and sector pattern forming applications to wireless ad hoc networks", IEE Proc.-Microw. Antennas Propag. Vol. 150, No. 4, pp. 203-208, August 2003..

[9] Y.Ojiro, H.Kawakami, K.Gyoda and T. Ohira, "Improvement of elevation directivity for ESPAR antennas with finite ground plane," Proc. IEEE 2001 Antennas Propagat. Soc. Symp.,Boston, MA, 2001, pp.18-19.

[10] J. Cheng, Y. Kamiya, and T. Ohira, "Adaptive beamforming of ESPAR antenna based on steepest gradient algorithm," IEICE Trans. Commun., vol.E84-B, pp.1790-1800, July 2001.

[11] B.Shishkov, J.Cheng, and T. Ohira, "Adaptive control algorithm of ESPAR antenna based on stochastic approximation theory," IEICE Trans. Commun., vol.E85-B, no.4, pp.802-811, Apr. 2002.